J. Phys. II France **5** (1995) 1193–1207 AUGUST **1995**, PAGE 1193

Classification
Physics Abstracts
42.70Df — 42.25Fx

On the Optics of Twist Grain Boundary Smectics

N. Andal and G.S. Ranganath

Raman Research Institute, Bangalore-560080, India

(Received 20 December 1995, revised 27 March 1995, accepted 21 April 1995)

Abstract. — We have studied theoretically the optical properties of twist grain boundary smectics. We find many reflection bands even at normal incidence. In some of the reflection bands an incident light in any state of polarization gets strongly reflected while in some others the strongly reflected state is of a circular polarization with the same or the opposite handedness as that of the structure. At oblique incidence, depending upon the screw symmetry, a reflection band either has three sub-bands of different polarizations or is a single band of a particular polarization. We find optical diffraction for light incident perpendicular to the twist axis. The diffraction pattern is completely different for TGB_A and TGB_C. In addition in absorbing TGB_C the pattern can even become asymmetric. From a Fourier inversion of the complex diffracted amplitudes we can evaluate in some cases the sizes of the smectic blocks and the grain boundaries.

1. Introduction

Twist grain boundary smectics (TGBS) have attracted a lot of attention in recent years [1,2]. The fact that these phases are rather analogous to the Abrikosov flux lattice found in Type II superconductors, has led to many investigations on these liquid crystals. Though most of the studies to date have been directed towards a study of their phase diagrams [3,4], attempts have also been made in the elucidation of their structures. In particular X-ray studies [5] on these phases have been quite rewarding. On the theoretical front, phenomenological descriptions [2] based on Landau models have been extensively used. From these studies, it has become clear that the TGBS are a helical stack of smectic blocks with the smectic layer normal perpendicular to the twist axis. Any two neighbouring smectic blocks or grains are connected through a twist grain boundary. Here also, as in crystals [6] the twist grain boundary is a periodic array of screw dislocations. The TGBS are classified as commensurate or incommensurate, depending upon whether or not the net director rotation across the grain is a rational multiple of 2π. In the case of commensurate TGBS, the twist axis also happens to be a N-fold screw axis, N being an integer. On the other hand, the incommensurate structures have no such screw symmetry. Further the smectic blocks could be of smetic A (S_A), smectic C (S_C) or smectic C* (S_{C^*}) structure. Then the TGBS are respectively designated as TGB_A, TGB_C and TGB_{C^*}.

Optical studies on TGBS structures have been largely confined to the determination of their pitch and the sense of the helix. Even here it has been tacitly assumed that these are akin

to cholesteric liquid crystals [7, 8]. In this paper we have worked out the optical reflection, transmission and diffraction properties of TGB_A and TGB_C. In the case of TGB_C the results are in general sensitive to the orientation of the local 2-fold axis with respect to the twist axis. For example the reflection spectrum and the diffraction pattern of a TGB_C structure with its local 2-fold axis parallel to the twist axis ($TGB_{C_{||}}$) are different from those found in a TGB_C having its local 2-fold axis perpendicular to the twist axis ($TGB_{C_\perp}$). Interestingly, we find that these liquid crystals are, optically, different from cholesterics and S_{C^*}. We get the following new results:

(a) The occurence of many reflection bands even at normal incidence. For a structure of a given handedness, in some bands, the polarization of the strongly reflected light can be either right circular or left circular. We also get bands wherein incident light of any polarization state gets strongly reflected. The former class of reflection bands are also associated with anomalous optical rotation while the latter class do not show optical rotation. In the case of absorbing TGBS, we get in some bands anomalous transmission of the strongly reflected state.

(b) For reflections at oblique incidence in the case of TGB_A (or $TGB_{C_{||}}$) for either even or odd values of N and in the case of $TGB_{C_\perp}$ for odd values of N, each reflection band has three sub-bands with different polarization features. But in the case of $TGB_{C_\perp}$ for even values of N, the primary and the higher order reflections corresponding to the full pitch do not have such a fine structure.

(c) For light incident perpendicular to the twist axis we get diffraction. The diffraction patterns of TGB_A and TGB_C are different both in intensity and polarization features. In TGB_A and $TGB_{C_{||}}$, which are optically like cholesterics, the diffraction pattern is similar to that of cholesterics.

(d) In the case of thin samples of non-absorbing TGB_A and $TGB_{C_{||}}$, the Fourier inversion of the complex amplitudes of the diffracted light leads to an evaluation of the sizes of the smectic blocks and the grain boundaries.

(e) In absorbing and non-absorbing TGB_A and $TGB_{C_\perp}$ the diffraction patterns are symmetric. On the other hand absorbing $TGB_{C_{||}}$ has an asymmetric diffraction pattern.

2. Model

The model of TGBS which we have used for our calculations is shown schematically in Figure 1. Optically the smectic blocks can be thought of as thick birefringent plates which are arranged in a uniform helical stack. Any two such neighbouring smectic blocks are connected by a grain boundary. In our model the grain boundary is approximated by a stack of thin birefringent plates. These thin plates smoothly rotate and connect the adjacent smectic blocks. Generally the size of the smectic block is of the order 1000 Å and that of the grain boundary is about 150 Å. As a further approximation to this model,we have also considered the case where the grain boundary is ignored altogether. Also, we must note that in TGB_A the blocks have uniaxial symmetry while in TGB_C the blocks have monoclinic symmetry. In the twist grain boundaries of both TGB_A and TGB_C we can assume, to a good approximation, local uniaxial symmetry. As a result of this both in the smectic blocks and the grain boundaries of TGB_A the index and absorption tensors are ellipsoids of revolution about the local director. On the other hand in TGB_C, in the smectic blocks the index and absorption tensors are triaxial ellipsoids. In these ellipsoids one of their principal axes will be along the local 2-fold axis and the other two will be at an angle with respect to one another. However, in the grain boundary of TGB_C the two tensors become ellipsoids of revolution about the local director.

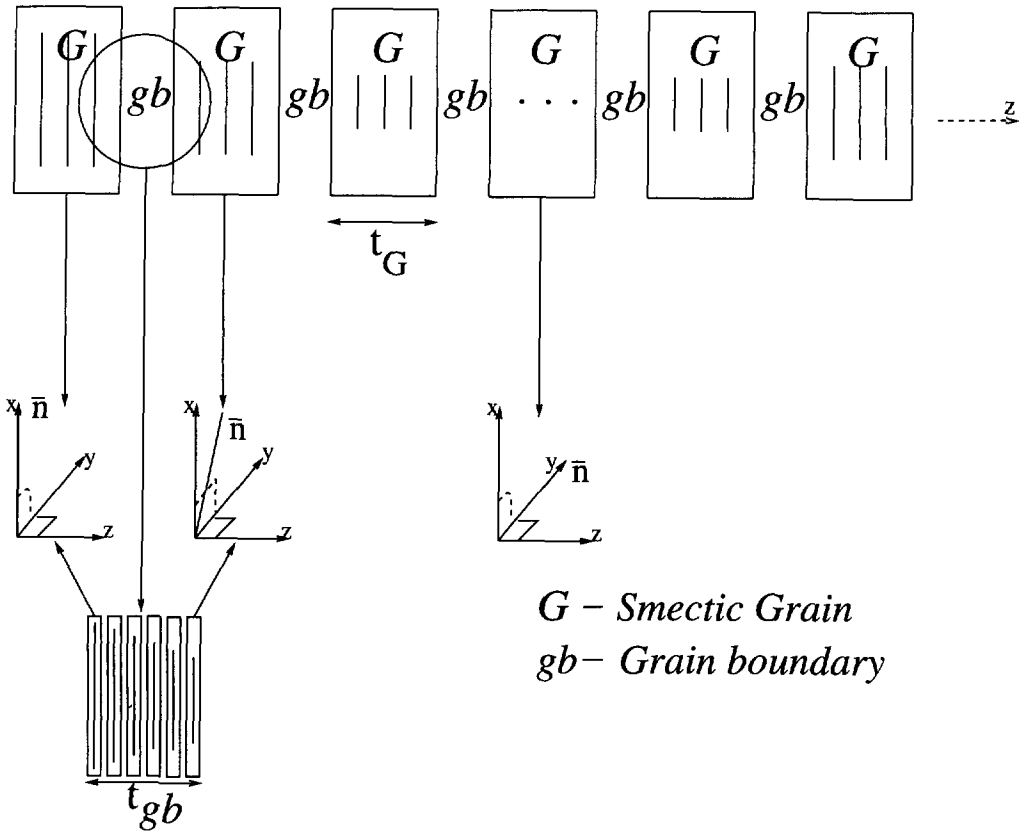

Fig. 1. — Schematic representation of the TGB_A model. The blocks denoted by G are the smectic grains. The grain boundary in between the grains is denoted by gb In both the smectic grains and the grain boundaries the projections of the director $\mathbf{n}$ in the (x, z) plane are shown. Here t_{gb} represents the thickness of the grain boundary and t_G is the thickness of the smectic block. The twist axis is along the z-direction We have shown here a left-handed structure.

3. Reflection and Transmission Spectra

3.1. THEORY. — We have worked out the optical reflection and transmission properties using the Berreman's 4×4 matrix formulation [9] of Maxwell's equations. Here the heterogenous anisotropic medium is divided into thin homogenous slabs, in each of which Maxwell's equations are solved. In any given slab

$$\frac{\partial \psi(z)}{\partial z} = \frac{\imath\omega}{c}\Delta(z)\psi(z) \tag{1}$$

where

$$\psi(z) = \begin{pmatrix} E_x \\ H_y \\ E_y \\ -H_x \end{pmatrix}$$

and $\Delta(z)$ is a 4×4 matrix whose elements contain the dielectric tensor components which are periodic in z. Here E_x, E_y and H_x, H_y are respectively the components of the electric and

magnetic fields in a plane perpendicular to the twist axis.
Integrating equation (1) we get

$$\psi(z) = M\psi(0). \tag{2}$$

The matrix M, called the propagation matrix, relates the field components in the $(j+1)^{\text{th}}$ slab to those in the j^{th} slab. The eigenvectors of M gives the modes which travel unaltered inside the medium. This method can be used to calculate the reflection spectrum, the transmission spectrum and the optical rotation. For non-absorbing systems the reflection and transmission spectra are complement to one another. It must be emphasised that in actual experiments we also have the bounding isotropic media. Then we use the method of Galatalo *et al.* [10], to calculate the eigenmodes which travel unchanged both in the liquid crystal and in the bounding media.

3.2. Results and Discussion

3.2.1. Normal Incidence

(a) Reflection Spectra

We find that a total reflection occurs at $\lambda = \mu p$ with p being the pitch of the structure and μ being its mean refractive index. This Bragg reflection has many features in common with the Bragg band seen in the cholesterics [11]. For example, a circularly polarized light of the same sense as that of the structure is totally reflected. The width of the reflection band is $p\delta\mu$ with $\delta\mu$ being the layer birefringence. Also the standing electromagnetic wave inside the reflection band has, locally, a linear polarization state. But unlike in cholesterics, the local electric vector of the standing wave does not follow the equivalent of the cholesteric director *viz.*, the smectic layer normal. However, globally the linear state rotates uniformly about the twist axis.

In contrast to cholesterics we get many reflection bands and the wavelengths at which they occur are decided by the symmetry of the screw axis. They occur at $\lambda = \mu p/m$ for $2, 4, 6...$ (N is even) screw symmetry and at $\lambda = 2\mu p/m$ for $1, 3, 5...$ (N is odd) screw symmetry, m being an integer. We can understand on a simple model,the positions and polarization featurs of the prominent reflections. A left handed structure of N-fold screw axis and of pitch p can also be looked upon as a right handed structure with a N'-fold screw axis with a pitch p'. Therefore, we can get from the same structure both right circularly polarized and left circularly polarized reflections. In the case of $N = 4$, however, both left and right have the same N-fold screw symmetry and hence in all the reflection bands this structure reflects both right circular and left circular polarizations. The positions of the interference maxima can be worked out by the so-called Kinematical Theory of Reflection from a helical stack of birefringent plates [12]. This procedure is also implied in the work of Joly et al concerning a helical stack of thick birefringent plates [13] ([1]). However, this method predicts only the positions at which reflection peak of a particular polarization occurs. For a knowledge of the intensity of reflections and the width of reflection bands, a theory taking into account multiple reflections is necessary. In our computation we have incorporated this feature explicitly.

A few computed reflection spectra are shown in Figure 2. We notice that neither reflections permitted for all values of m are seen nor the intensities of the different reflections are the same. Another important feature of these reflections is that in some of them circularly polarized light of the same sense as that of the helix is strongly reflected and in some others circularly polarized light of the opposite sense is strongly reflected. In view of this, the determination of the pitch and the sense of the helix could be completely wrong if we happen to treat any of these higher order reflections as a cholesteric reflection. Interestingly there are also reflections wherein an

([1]) We are thankful to a referee for comments on this point.

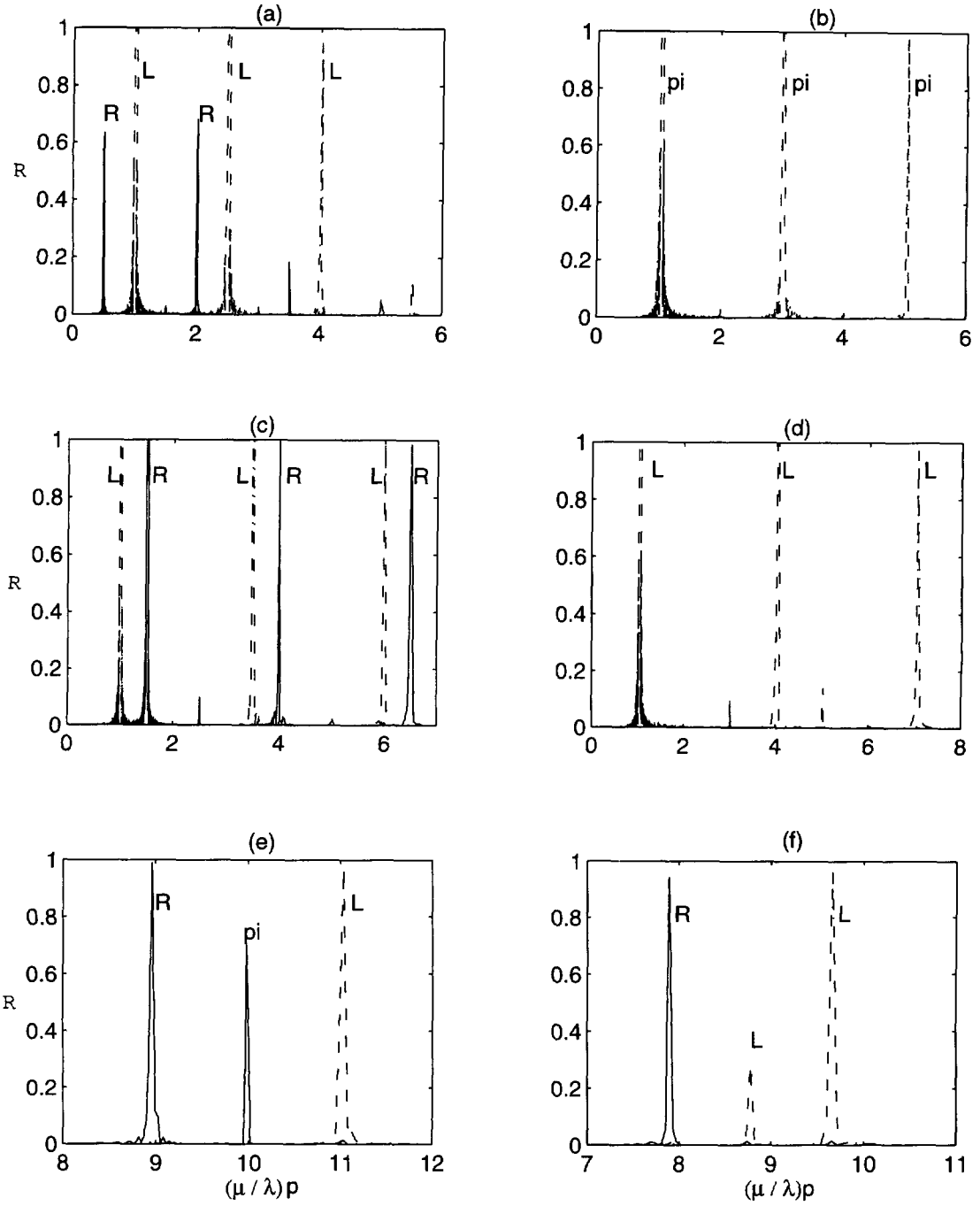

Fig 2. — The reflectance (R) as a function of ($\mu p/\lambda$). Smectic block thickness t_G = 1000 Å, grain boundary thickness t_{gb} = 150 Å and inter-grain angle is 18°. a) $N = 3$; b) $N = 4$; c) $N = 5$; d) $N = 6$, e) $N = 20$ and f) incommensurate TGB_A with an inter-grain angle of nearly 18° and here p denotes the pitch of the nearest commensurate structure of inter-grain angle of 18° exact. Here R and L represent the right and left circularly polarized state, respectively, and *pi* represents the polarization insensitive reflection. Throughout this paper computations have been made for a left handed-structure.

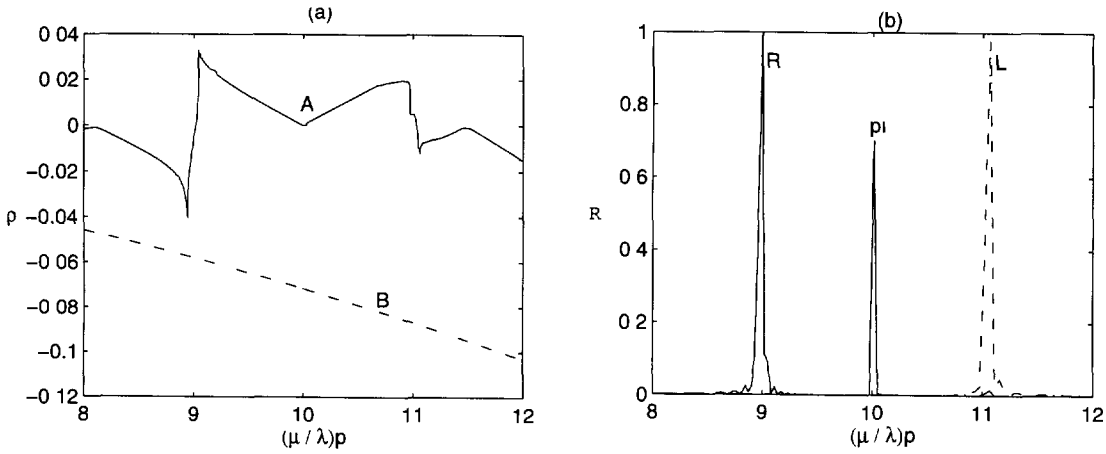

Fig 3. — a) Rotatory power (ρ) as a function of ($\mu p/\lambda$). Here A is for TGB_A and B is for a cholesteric with same parameters but using de Vries formula, b) higher-order reflection spectrum of TGB_A in the same ($\mu p/\lambda$) range.

incident light in any state of polarization gets strongly reflected in the same state. Here it may be mentioned that for the 4-fold screw symmetry, i.e., $N = 4$, all the reflections are of this latter type, i.e., they are polarization insensitive.

(b) Incommensurate Structures

If the structure is incommensurate the spectrum gets considerably altered. In Figure 2f, we give the higher order reflection spectrum for an inter-grain twist of nearly 18°. In fact the twist is $2\pi\alpha$, α being an irrational number close to 0.05. This spectrum is quite different from that shown in Figure 2e which corresponds to an inter-grain angle of exactly 18°. We note that the reflections do not any more occur exactly at $\lambda = \mu p/m$. Also, interestingly in this example, the polarization insensitive band is absent.

(c) Anomalous Optical Rotation

As in cholesterics here also the base states are right and left circular polarizations travelling with different velocities. Hence the structure has optical rotation. As one approaches a band of either left or right circular reflection, the optical rotatory power increases and changes sign on crossing the band, i.e., the rotation becomes anomalous. The rotation anomaly in a band associated with the reflection of right circularly polarized light is opposite in sign to that found in a band associated with the reflection of left circularly polarized light. Also we find that the rotatory power in the wavelength range of the higher order reflection bands does not obey the de Vries formula for cholesterics [14]. It may be noticed that the difference is both in sign and in magnitude. All these features are depicted in Figure 3. Hence even a study of optical rotation cannot lead to an unambiguous determination of pitch or helical sense.

(d) Effect of Structural Parameters

In view of the structural similarities that TGBS have with the Abrikosov flux lattice, we can expect the smectic order parameter to gradually decrease and finally vanish as one enters the grain boundary. As a result of this the director twist in the grain boundary will be non-uniform. Lubensky and Renn [2] predict a Gaussian variation of the order parameter. Using this fact and a simple model we calculated the non-uniform director twist. Optical calculations based on this model were compared with those carried out on a less realistic model where we assume a uniform director twist in the grain boundary. For all practical purposes the model, with grain

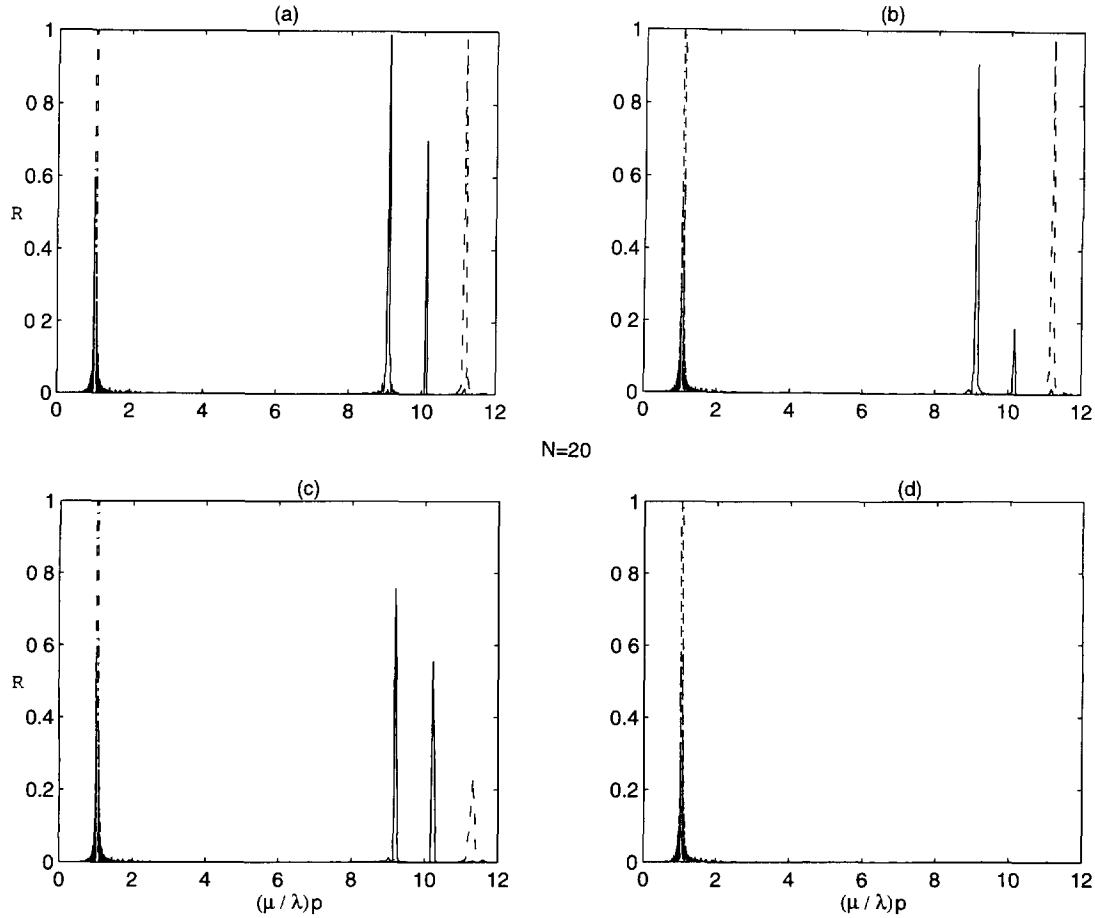

Fig 4 — Reflection spectra of TGB_A with $N = 20$ for a grain boundary thickness of 150 Å and for different thicknesses of the smectic block: a) 750 Å; b) 500 Å, c) 300 Å and d) 100 Å

boundaries of uniform twist, appeared good enough. In our simplified model the total twist in the grain boundary is comparable to that in a normal cholesteric of equivalent thickness (i.e., its pitch is about 0.3 microns or more).

We now consider the influence of the thickness of the smectic block. In Figure 4 we give the reflection spectra for a TGB_A (or $TGB_{C_{||}}$) with an inter-grain angle of 18° ($N = 20$) computed for different thicknesses of the smectic block keeping the grain boundary thickness the same. We find that when the smectic block thickness is less than about 150 Å, the spectrum goes over to that of a cholesteric, i.e., only one reflection band. Similarly in the case of $TGB_{C_\perp}$ the spectrum goes over to that of S_{C^*} of a high tilt angle. This effect is true for only small inter-grain angles irrespective of the value of N.

We have also considered a simplified model of TGBS where we ignore its grain boundaries. We find that this model gives a very different reflection spectrum for intergrain angle greater than or equal to 90°. In Figure 5 this difference has been brought out for a TGB_A of a 3-fold screw symmetry. In this context it may be mentioned that Joly and Isaret [13] have studied, using a 2×2 matrix formulation the reflection spectra for helical stacks of birefringent plates

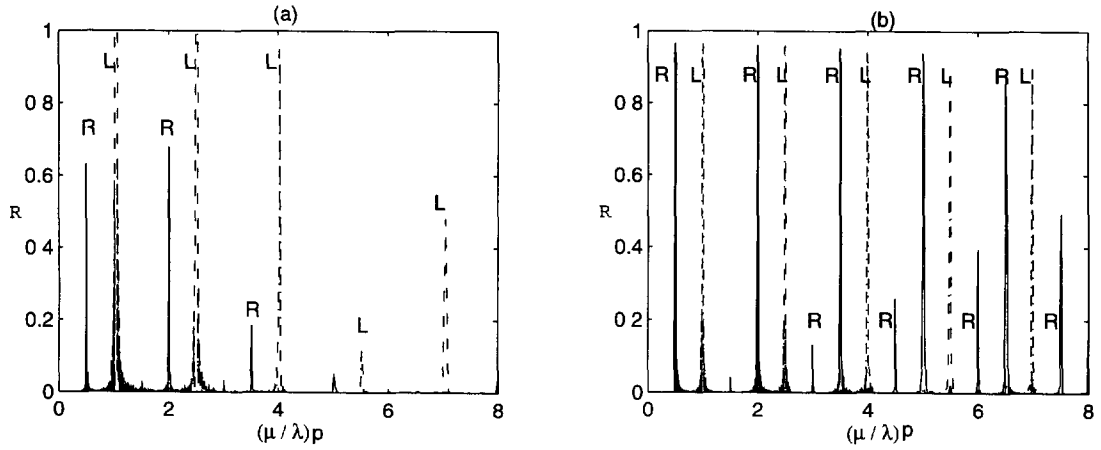

Fig. 5. — Reflection spectra of TGB_A for $N = 3$, a) with the grain boundary; b) without the grain boundary.

of very high phase retardation. Some of the features of the TGBS are present in their systems.

3.2.2. Oblique Incidence. — In this geometry also the reflection spectrum is decided by the screw symmetry. In the case of $2, 4, 6...$ (even N) screw symmetry both for TGB_A and $TGB_{C_{||}}$, reflection peaks occur at $\mu p/\lambda = m$ while for $TGB_{C_\perp}$ they occur at $\mu p/\lambda = m/2$. In Figure 6a we give the spectrum computed for TGB_A and in Figure 6b that for $TGB_{C_\perp}$. However for $1, 3, 5...$ (odd N) screw symmetry, the three TGBS, namely TGB_A, $TGB_{C_{||}}$ and $TGB_{C_\perp}$ have reflections at $\mu p/\lambda = m/2$. This is shown in Figure 6c for TGB_A and in Figure 6d for $TGB_{C_\perp}$. It may be remarked that it is not easy to extend for this case the simple Kinematical explanation presented for normal incidence. In particular, it is difficult to account for the presence of sub-bands whose polarization features are sensitive functions of the tilt-angle θ and birefringence.

As in the case of normal incidence, here also reflections at all permitted values of m are not present. Also, in TGB_A or $TGB_{C_{||}}$ for even or odd values of N and $TGB_{C_\perp}$ for odd values of N, for angles of incidence greater than about 30° each Bragg band splits up into three sub-bands with different polarization properties. We find that in the lower wavelength sub-band an incident wave with its electric vector perpendicular to the plane of incidence (TE) gets reflected in the same state (TE). On the other hand in the longer wavelength sub-band a wave with its electric vector parallel to the plane of incidence (TM) gets reflected in the same state (TM). In the central sub-band a wave in the TM state gets reflected in the TE state and *vice versa*. This is explicitly shown in Figure 6e for one such band.

On the other hand, surprisingly for $TGB_{C_\perp}$ for even values of N, we get new reflections at oblique incidence corresponding to half integral values of $\mu p/\lambda$ and they do not split into sub-bands. And in such bands, an incident TE state is reflected as a TM state and vice-versa. One such band is also shown in Figure 6e. Interestingly the polarization features of the three sub-bands shown in Figure 6e are rather similar to those found in cholesterics and are quite different from those of normal S_{C^*}. We have shown in Figure 6f a typical S_{C^*} reflection. This difference is due to the fact that in all the three TGBS considered here, the molecular tilt with respect to the twist axis is quite large. Thus this structure has optical properties that were predicted by Oldano [15] for a S_{C^*} with a tilt angle above a certain value θ_c. As was first

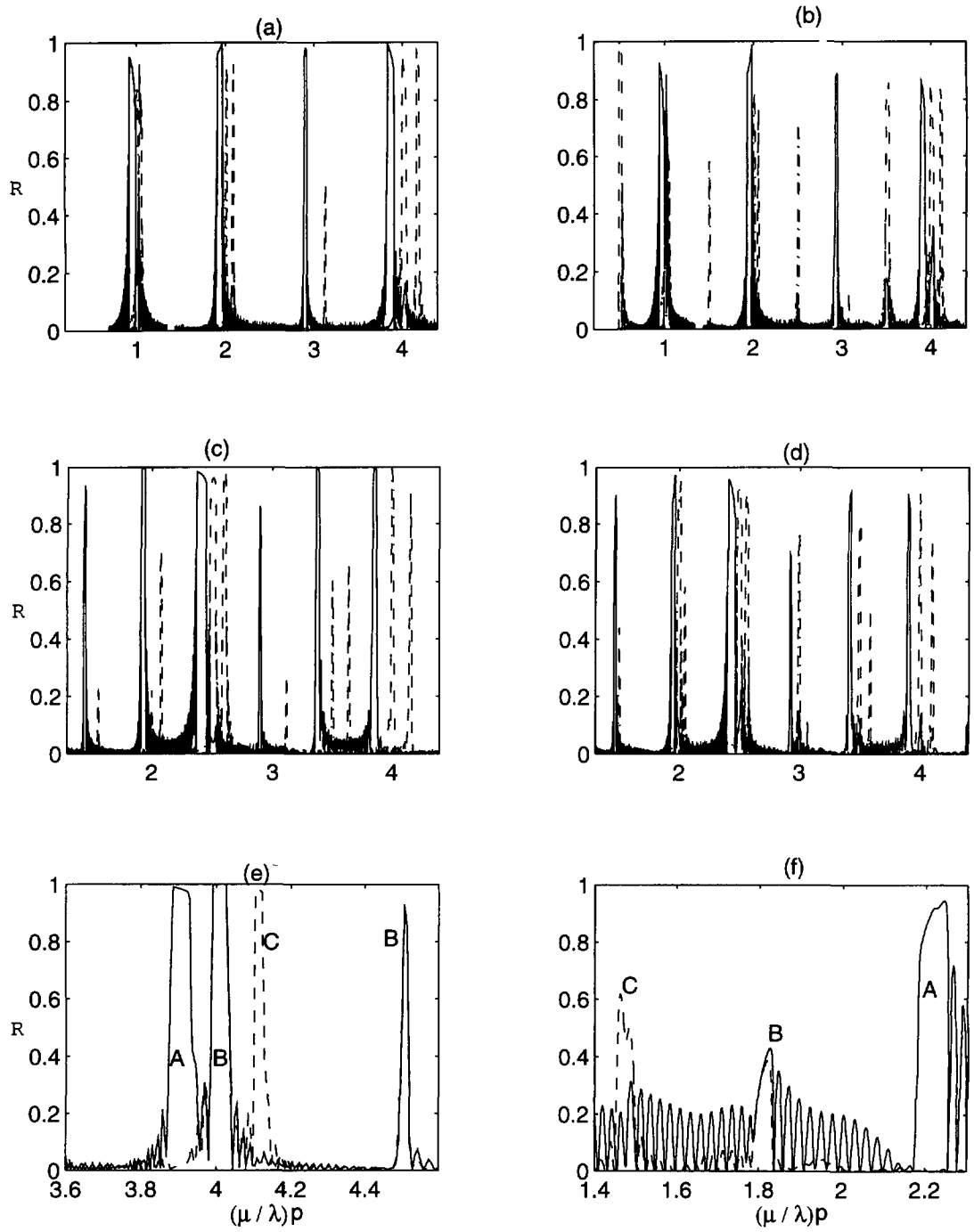

Fig. 6. — Reflection spectra at an angle of incidence of 60°: a) Reflection peaks occur at integral values of $(\mu p/\lambda)$ for TGB_A with $N = 6$; b) Reflection peaks occur at integral and half integral values of $(\mu p/\lambda)$ for a $TGB_{C_\perp}$ with $N = 6$. Reflection spectrum of c) TGB_A and d) $TGB_{C_\perp}$ for $N = 3$ have half integral reflections in both. Polarization features of a reflection band of e) $TGB_{C_\perp}$ with $N = 6$ and *(f)* S_{C^*}. *Here A represents incident TE state reflected as a TE state,* B represents incident TE (or TM) state reflected as a TM (or TE) state and C represents incident TM state reflected as TM state.The tilt angle with respect to the twist axis is 18° in S_{C^*} and 72° in $TGB_{C_\perp}$

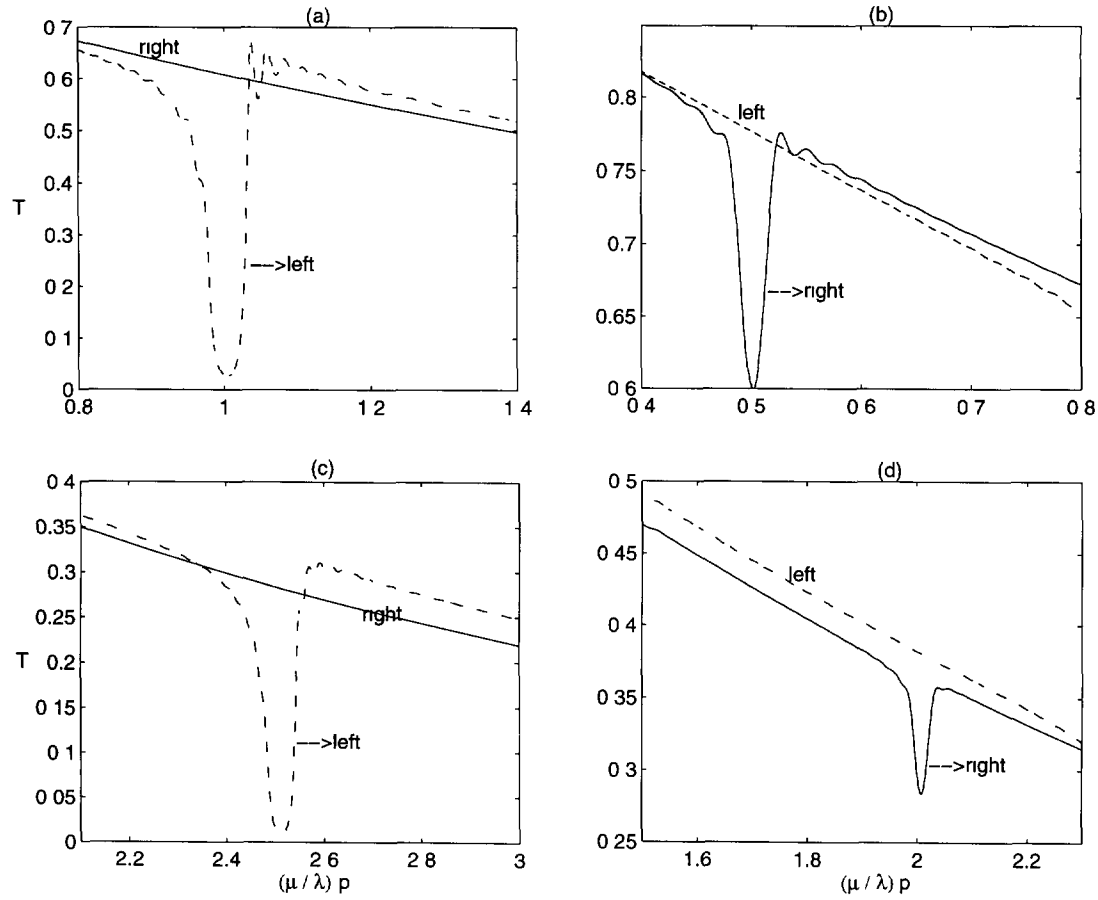

Fig. 7. — Transmission spectra of TGB_A with $N = 3$ showing the transmittance T as a function of $(\mu p/\lambda)$: a) and b) the anomalous transmission is on the shorter wavelength side of the reflection band; c) the anomalous transmission occurs at both the short and long wavelength sides of the reflection band; d) the anomalous transmission is absent throughout the band.

shown by him, an S_{C^*} with a tilt angle greater than θ_c is optically different from an S_{C^*} with a tilt angle less than θ_c , in that the short wavelength and long wavelength sub-bands have oppposite polarization features in the two cases. In conclusion we notice that oblique reflection studies can distinguish between $TGB_{C_\perp}$ and TGB_A or $TGB_{C_{||}}$.

3.2.3. Effects of Absorption

(a) Transmission Spectra

In the case of absorbing cholesterics, the reflection band is associated with anomalous transmission or Bormann effect [16]. Bormann effect is also possible in absorbing TGBS but only in the bands associated with the reflection of a circular state This is shown in Figure 7 for a TGB_A with $N = 3$. In every reflection band the circular state which does not suffer reflection is transmitted with an average absorption. However , the reflected circular state is transmitted with a relatively higher intensity. This anomalous transmission or Bormann effect is on the shorter wavelength edge of the reflection band as shown in Figure 7a for a band reflecting

left circularly polarized light and in 7b for a band reflecting right circularly polarized light. Interestingly, there are some reflection bands in which the anomalous transmission occurs at both the short and long wavelength edges as shown in Figure 7c. Further we also get reflection bands in which the Bormann effect is altogether absent as shown in Figure 7d. For the parameters considered in our computations all the three types of transmissions are seen for $N = 3$. On the other hand for other values of N, we generally get only one or two of the three types of transmissions. We get similar results in the case of $TGB_{C_\perp}$ also.

(b) Reflection Spectra

In absorbing systems. the reflection and transmission spectra are not complementary. Just as in absorbing cholesterics [17], even here a peak in the reflection spectrum is also a peak in the transmission spectrum. Further we find that there are not any marked differences in $TGB_{C_{||}}$ or $TGB_{C_\perp}$ due to its local biaxiality. Even here with reflection spectra we can distinguish between the three different TGBS .

4. Optical Diffraction

4 1. THEORY. — When light is incident perpendicular to the twist axis of TGBS, in general we find diffraction. This is due to the fact that the medium acts as a phase grating. An incident plane wavefront gets corrugated inside the medium leading to diffraction. Here again we have used the model described in Section 2.

4.1.1. Non-Absorbing Case

(a) Thin samples

In TGBS, if the sample thickness or the birefringence is small enough so that internal diffractions can be ignored then the generalised Raman-Nath theory (RN) [18] can be used. Both TGB_A and $TGB_{C_{||}}$ have similar diffraction patterns with diffraction peaks at angles Θ given by

$$\Theta = \pm \sin^{-1}(2m\lambda/\mu p) \tag{3}$$

Also diffraction takes place only for the component of the electric vector perpendicular to the twist axis. At any diffraction angle Θ the diffracted amplitude is given by

$$U(\Theta) = \int_{-\infty}^{\infty} \exp(-i\frac{2\pi z}{\lambda}\sin\Theta)[\exp(i\frac{2\pi t}{\lambda}\mu(z))]\mathrm{d}z \tag{4}$$

where

$$\frac{1}{(\mu(z))^2} = \frac{(\sin(\psi(z)))^2}{\mu_e^2} + \frac{(\cos(\psi(z)))^2}{\mu_o^2} \tag{5}$$

Here μ_o and μ_e are the local ordinary and the extraordinary refractive indices, $\psi(z)$ the orientation of the local director and t is the sample thickness. In principle we can experimentally extract $U(\Theta)$ both in amplitude and phase. Then from equation (4) through a Fourier inversion, we can get $\mu(z)$ or equivalently $\psi(z)$. From the structure of TGBS it is obvious that $\psi(z)$ is constant in the smectic block and varies with z, only in the grain boundary. Hence $\psi(z)$ profile leads to an evaluation of the thickness of the smectic block and that of the grain boundary. Also this method will reveal the nature of the director twist present inside the grain boundary.

(b) Thick samples

When the sample is thick, internal diffractions become important and to incorporate this we use the Rokushima-Yamakita theory (RY) [19]. In this theory the **E** and **H** vectors of the incident electromagnetic wave and the components of the dielectric tensor are expressed as Fourier sums with weighted coefficients. The Maxwell's equations in the RY notation become:

$$\frac{\mathrm{d}}{\mathrm{d}\overline{x}} f_{\hat{t}} = iC f_{\hat{t}} \tag{6}$$

$$f_{\hat{n}} = D f_{\hat{t}} \tag{7}$$

with $\overline{x} = x\omega/c$. Here

$$f_{\hat{t}} = \begin{pmatrix} \tilde{e_y} \\ \tilde{h_z} \\ \tilde{e_z} \\ \tilde{h_y} \end{pmatrix} \quad \text{and} \quad f_{\hat{n}} = \begin{pmatrix} \tilde{e_x} \\ \tilde{h_x} \end{pmatrix}$$

are respectively the tangential and normal components of the fields at the interfaces. Also $\tilde{e_i} = \tilde{e_i}(\overline{x})$ and $\tilde{h_i} = \tilde{h_i}(\overline{x})$ are infinite column matrices with elements $e_{im}(x)$ and $h_{im}(x)$, m being an integer. These elements are the Fourier components of E_i and H_i, respectively. The coupling matrices C and D are given by

$$C = \begin{pmatrix} 0 & -1 & 0 & 0 \\ \varepsilon_{yx}\varepsilon_{xx}^{-1}\varepsilon_{xy} - \varepsilon_{yy} + \tilde{\mathbf{q}}^2 & 0 & 0 & -\varepsilon_{yx}\varepsilon_{xx}^{-1}\tilde{\mathbf{q}} \\ \tilde{\mathbf{q}}\varepsilon_{xx}^{-1}\varepsilon_{xy} & 0 & 0 & -\tilde{\mathbf{q}}\varepsilon_{xx}^{-1}\tilde{\mathbf{q}} + \mathbf{1} \\ 0 & 0 & \varepsilon_{zz} & 0 \end{pmatrix}$$

$$D = \begin{pmatrix} -\varepsilon_{xx}^{-1}\varepsilon_{xy} & 0 & 0 & \varepsilon_{xx}^{-1}\tilde{\mathbf{q}} \\ -\tilde{\mathbf{q}} & 0 & 0 & 0 \end{pmatrix}$$

Here,
ε_{ij} (i,j = x,y,z) are $(2m+1) \times (2m+1)$ sub-matrices with elements
$\varepsilon_{ij,nl} = \varepsilon_{ij,n-l}$, the $(n-l)^{th}$ Fourier component of ε_{ij}
$\tilde{q} = \delta_{nl} q_l$
$q_l = lq + q_0$
$q = 2\pi/p$ and $q_o = n_i \sin\beta$
n_i is the refractive index of the first bounding medium and β is the angle of incidence.
The diffraction results from the coupling of the TM and TE modes through C.

4.1.2. Absorbing Case. — In this case, absorption attenuates considerably the intensity of the diffracted light. Hence only studies on thin samples will be meaningful and in this limit the RN theory can be used.

4.2. Results and Discussion

4.2.1. Non-Absorbing Case. — Diffraction pattern has been worked out for thick samples. In Figure 8a we give a computed diffraction pattern of TGB_A. An essentially similar pattern is seen for $TGB_{C_{||}}$. It is seen to be symmetric. It must be remarked that the intensity of any order

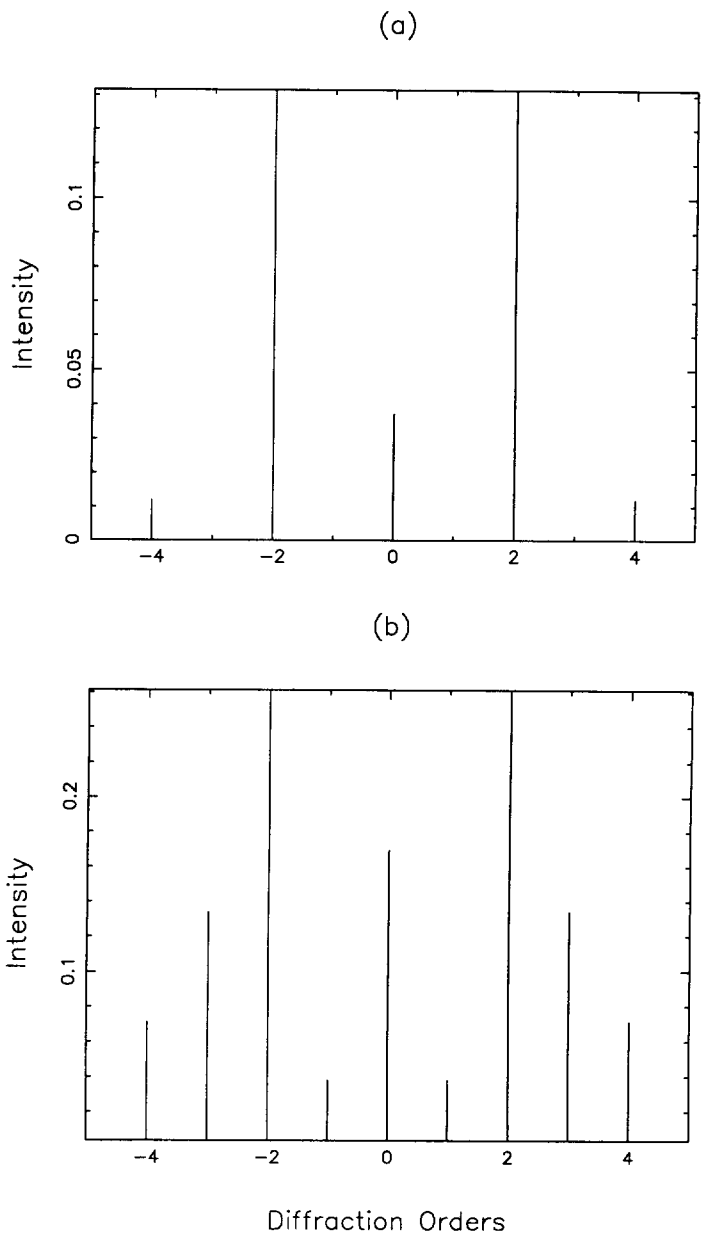

Fig. 8. — A typical diffraction pattern in the phase grating mode, a) TGB_A (or $TGB_{C_{||}}$) and b) $TGB_{C_\perp}$, computed for a sample thickness of 20 μ.

is a sensitive function of sample thickness. Also in TGB_A or $TGB_{C_{||}}$ for an incident light at any general azimuth the central order is elliptically polarized while all the higher diffraction orders are nearly linearly polarized perpendicular to the twist axis . On the other hand no diffraction takes place for incident light polarized parallel to the twist axis. However, in $TGB_{C_\perp}$ we get *diffraction for any azimuth of the incident light*. The pattern has extra orders which happen to be the odd orders of diffraction. In Figure 8b we give the computed diffraction pattern for

Fig. 9. — Diffraction pattern for an absorbing $TGB_{C_{||}}$. The angle between the elliptic sections of the index and absorption ellipsoids is 45°. The birefringence $\Delta n = 0.1$ and the dichroism $\Delta k = 0.003$.

$TGB_{C_\perp}$. In any given order the polarization is dependant on the incident polarization and the thickness of the sample just as in S_{C^*} [20]. Thus we cannot differentiate between TGB_A and $TGB_{C_{||}}$. But these two can be differentiated from $TGB_{C_\perp}$. It must be noted that in all these cases the diffraction pattern is symmetric. If the structures are incommensurate then they become quaziperiodic. In such structures there are very many diffraction orders and each order will have to be described by a pair of integers [20, 21]. We can expect a very similar behaviour even here.

4.2.2. Absorbing Case. — The diffraction patterns of thin TGB_A and $TGB_{C_\perp}$ continue to be symmetric even in the absorbing case. However, surprisingly, in thin absorbing $TGB_{C_{||}}$ the pattern is asymmetric. This asymmetry is due to the relative tilt between the central elliptic sections perpendicular to the common two-fold axis of the absorption and the index ellipsoids. The diffraction pattern computed for a relative tilt of 45° is shown in Figure 9. It is therefore possible to distinguish between TGB_A and $TGB_{C_{||}}$ if they are absorbing. It may be remarked that the diffraction pattern becomes symmetric when the angle between elliptic sections is either equal to 0° or 90°. Thus we find that from a study of diffraction we can distinguish between the three TGBS *viz.*, TGB_A, $TGB_{C_{||}}$ and $TGB_{C_\perp}$.

5. Conclusion

A study of the optical properties of twist grain boundary smectics (TGBS) has been undertaken both in the Bragg and the phase grating modes. The TGBS give higher order Bragg reflections.

They exhibit anomalous optical rotation and transmission. Generally at oblique incidence the reflection bands split into three sub-bands with different polarizational features. In the phase grating mode we have considered both thin and thick samples of TGBS. In thin samples Fourier inversion of the diffracted amplitudes yields the smectic block and grain boundary thicknesses. It is shown that a study of the reflection spectra can differentiate only between TGB_A(or $TGB_{C_{||}}$) and $TGB_{C_\perp}$ while a study of the diffraction pattern can differentiate all the three TGBS.

Acknowledgments

Our thanks are due to K A. Suresh for useful discussions.

References

[1] Goodby J W., Waugh M.A , Stein S.M , Chin E., Pindak R. and Patel J.S , *Nature* **337** (1989) 449.

[2] Lubensky T C. and Renn S R , *Phys. Rev. A* **41** (1990) 4392.

[3] Renn S.R , *Phy Rev A* **45** (1992) 953.

[4] Renn S.R and Lubensky T.C., *Mol Cryst. Liq. Cryst* **209** (1991) 349.

[5] Navailles L , Barois P and Nguyen H.T., *Phy. Rev. Lett* **71** (1993) 545.

[6] Cottrell A , Dislocations and Plastic Flow in Crystals (Oxford, 1953).

[7] Srajer G., Pindak R., Waugh M.A , Goodby J W. and Patel J.S , *Phys Rev. Lett* **64** (1990) 1545

[8] Yanoff B.D , Ruether A.A , Collings P.J , Slaney A J. and Goodby J W., *Liq. Cryst.* **14** (1993) 1794.

[9] Berreman D.W., *J Opt Soc. Am.* **62** (1972) 502.

[10] Galatola P., Oldano C. and SunilKumar P.B., *J. Opt. Soc. Am.* **A11** (1994) 1332.

[11] Belyakov V.A. and Dmitrienko V.E., Soviet Scientific Reviews – Section A, Vol. 13, Part 1, I.M. Khalatnikov, Ed. (Harwood Academic Publishers, London, 1989).

[12] Chandrasekhar S. and Ranganath G.S., *Mol Cryst. Liq. Cryst.* **25** (1974) 195.

[13] Joly G. and Isaret N., *J Optics (Paris)* **17** (1986) 211

[14] de Vries H., *Acta Cryst.* **4** (1951) 219.

[15] Oldano C , *Phys Rev Lett* **53** (1984) 2413.

[16] Suresh K.A., *Mol. Cryst. Liq. Cryst* **35** (1976) 267.

[17] Sah Y. and Suresh K.A., *J Opt Soc. Am.* **A11** (1994) 740.

[18] Suresh K.A., SunilKumar P.B. and Ranganath G.R., *Liq. Cryst.* **11** (1992) 73.

[19] Rokushima K. and J. Yamakita, *J. Opt. Soc. Am.* **73** (1983) 901.

[20] Suresh K.A., Sah Y , SunilKumar P.B. and Ranganath G.S , *Phys. Rev. Lett.* **72** (1994) 2863

[21] Mosseri R. and Bailly F., *J. Phys. I France* **2** (1991) 1715.

[22] Sah Y. and Ranganath G S., *Opt. Commun.* **114** (1995) 18